



Heterogeneous reactions between NO₂ and anthracene adsorbed on SiO₂ and MgO

Jinzhua Ma, Yongchun Liu, Hong He*

State Key Laboratory of Environmental Chemistry and Ecotoxicology, Research Center for Eco-Environmental Sciences, Chinese Academy of Sciences, Beijing 100085, China

ARTICLE INFO

Article history:

Received 27 July 2010

Received in revised form

3 November 2010

Accepted 10 November 2010

Keywords:

PAH

Anthracene

Mineral oxides

NO₂

Kinetics

Oxidation products

ABSTRACT

The heterogeneous reactions of NO₂ with anthracene adsorbed on SiO₂ and MgO were investigated under dark conditions at 298 K using DRIFTS, GCMS, and UV–Vis. The pseudo-first-order rate constants of anthracene on SiO₂ and MgO were obtained by fitting the exponential decay of adsorbed PAH concentrations versus reaction time. The reaction on SiO₂ was almost two times faster than on MgO when the concentration of NO₂ was 3.69×10^{12} molecules cm⁻³. Both 9-nitroanthracene and 9,10-anthraquinone were the products of the nitration of anthracene adsorbed on SiO₂ whereas 9,10-anthraquinone was the only product formed by NO₂ reaction with anthracene adsorbed on MgO. These results suggest that mineral oxides not only control the reaction kinetics of PAHs with NO₂ but also alter the reaction pathway for the heterogeneous reaction of PAHs with NO₂. The difference in the heterogeneous reactivity of NO₂ with anthracene adsorbed on SiO₂ and MgO was ascribed to the formation of HNO₃ on SiO₂, which can catalyze the nitration of PAHs by NO₂. Due to the formation of nitro-anthracene and oxy-anthracene, the heterogeneous reactions of NO₂ with anthracene also altered the optical properties of the mineral oxides on which anthracene were adsorbed.

© 2010 Elsevier Ltd. All rights reserved.

1. Introduction

Polycyclic aromatic hydrocarbons (PAHs) mainly originate from incomplete combustion of fossil fuels (petroleum, natural gas, and coal) and biomass burning. The global emission of atmospheric PAHs is roughly estimated to be 0.001–0.02 TgC yr⁻¹ and about 90% of PAHs emissions are anthropogenic (Calvert et al., 2002). As ubiquitous persistent organic pollutants (POPs), PAHs and their derivatives (nitro-PAHs, oxy-PAHs, etc.) have attracted much attention due to their allergenic, mutagenic, and carcinogenic properties (Finlayson-Pitts and Pitts, 1997). In particular, nitro-PAHs have been identified as a class of very potent mutagenic compounds from environmental samples (Feilberg et al., 2001; Albinet et al., 2006; Pitts et al., 1985a; Ramdahl et al., 1986; Xu and Jin, 1984). The concentration levels range from <1 pg m⁻³ to ~1 ng m⁻³ and are usually a factor of 10–1000 below the parent PAHs concentrations (Feilberg, 2000). However, nitro-PAHs are typically 100,000 times more mutagenic and 10 times more carcinogenic than the corresponding parent PAHs (Onchoke et al., 2009). For these reasons it is necessary and important to identify the sources of nitro-PAHs in the atmosphere.

The presence of nitro-PAHs in environmental samples may be due to their occurrence in emissions from the above mentioned sources or by homogeneous and heterogeneous reactions in the atmosphere (Pitts et al., 1978). In the gas phase, nitro-PAHs can form by the reaction of PAHs with NO₃ or OH in the presence of NO₂ (Atkinson and Arey, 1994; Atkinson et al., 1987; Bunce et al., 1997). The reactions of PAHs adsorbed on soot (Kamens et al., 1990) or glass fiber filters (Pitts et al., 1985b) with N₂O₅ or HNO₃ also lead to the formation of nitro-PAHs. Heterogeneous reactions of PAHs adsorbed on particles with NO₂ may also be an important source of nitro-PAHs. For example, Kwamena and Abbatt (2008) found that nitration of pure anthracene and pyrene by NO₂ (406 ppb) or HNO₃ (284 ppm) under dark conditions does not occur at room temperature and ambient pressure. However, Wu and Niki (1985) revealed that the half-life of pyrene on silica plates with 1 ppm of NO₂ in N₂ was only 1.4 h at 298 K. These results imply that the substrate plays an important role in the heterogeneous reaction of PAHs with NO₂. Ramdahl and Bjørseth (1984) studied the heterogeneous reactions of PAHs adsorbed on SiO₂, Al₂O₃, and charcoal particles with NO₂ (0.5 ppm) and found that the yield of nitro-PAHs on SiO₂ was higher than on Al₂O₃, which means SiO₂ has a more reactive surface than Al₂O₃. The rate constants for the heterogeneous reaction of NO₂ with various PAHs depended on the structure of the PAHs on SiO₂ particles (from 4×10^{-8} to 1.4×10^{-3} s⁻¹ (Perraudin et al., 2005)), while the rate constants were in the same order of magnitude for

* Corresponding author. Tel.: +86 10 62849123; fax: +86 10 62923563.
E-mail address: honghe@rcees.ac.cn (H. He).

different PAHs on graphite (from 2.0×10^{-3} to $8.4 \times 10^{-3} \text{ s}^{-1}$ (Esteve et al., 2004)) or diesel exhaust particles (from 1.7×10^{-3} to $3.2 \times 10^{-3} \text{ s}^{-1}$ (Esteve et al., 2006)). These results suggest that the reactivity of PAHs with NO_2 on the surface may greatly depend on the nature of the substrates. However, it is unclear that what the essence for this substrate effect is.

Mineral dust, which mainly originates from arid and semi-arid regions with global source strength of about 1000–3000 Tg yr^{-1} (Dentener et al., 1996), is one of the most important contributors to the loading of atmospheric particle matters. In the atmosphere, PAHs are able to partition between the gas phase and atmospheric particulate matter. Recently, field measurements also found that PAHs usually adsorb on mineral dust in real atmospheric particulate matter (Wu et al., 2005; Fu et al., 2009). Therefore, it is very significant to investigate the chemical behavior of PAHs on mineral dust. Unfortunately, the mechanism for how mineral dust affects the heterogeneous reactions of PAHs with NO_2 remains unclear. The reaction of NO_2 with anthracene adsorbed on MgO has never been carried out. In this study, we selected SiO_2 and MgO as model mineral particles and anthracene as the representative PAH compound to investigate the effect of mineral substrates on the heterogeneous reaction of PAHs with NO_2 . The results will help understand the chemical behavior of PAHs and the source of nitro-PAHs in the atmosphere.

2. Experimental

2.1. Particles and characterization

The SiO_2 sample was prepared from SiO_2 (Degussa 304N) by calcining at 1273 K for 3 h. The MgO sample was supplied by Haizhong Chemicals Plant in Tianjin. The specific surface area of these samples was measured using Nitrogen Brunauer–Emmett–Teller (BET) physisorption (Quantachrome Autosorb-1-C). The crystalline phase for these samples were identified to be amorphous (SiO_2) and periclase (MgO) by a D/max-RB automatic powder X-ray diffractometer (XRD) using $\text{Cu K}\alpha$ irradiation.

2.2. Sample preparation and storage

Before adsorption of anthracene, SiO_2 and MgO were cleaned three times by ultrasonication in dichloromethane (Chromatographic Grade), followed by drying at room temperature. The concentration of PAHs in the extract of cleaned particles and the pure solvent can not be detected by the gas chromatography–mass spectrometer (Agilent 6890/5973).

Anthracene was adsorbed on particles by the impregnation method. Approximately 1.0 g of cleaned particles was added to 20.0 mL of n-hexane (Chromatographic Grade) containing 500 μg of anthracene. After stirred homogeneously, the solvent was slowly evaporated using a rotary evaporator at 303 K. Finally, the particles were dried at room temperature for 4 h. To avoid the photo-degradation of adsorbed PAHs, all particles were stored in amber glass flasks at 255 K in dark.

2.3. Reaction procedure and analytical methods

All experiments were performed under dark conditions at 298 K. A total of 20.0 mg of coated particles were evenly deposited on a Teflon disc (the geometric surface area is 3.39 cm^2), which was then placed in a quartz reactor. In the case of reaction on Teflon disc, 1.16 μg of anthracene dissolved in CH_2Cl_2 was evenly distributed on the Teflon disc. Before NO_2 was introduced into the quartz reactor, $\text{O}_2/\text{NO}/\text{N}_2$ with a given concentration was flowed through another blank reactor. The concentration of NO_2 was analyzed by an online

Nexus 6700 FT-IR spectrometer equipped with a gas cell having an optical length of 2 m. When the concentration of NO_2 was stable, the feed gas was switched to the reactor containing adsorbed anthracene for reaction.

The reacted particle samples were ultrasonically extracted using 20.0 mL CH_2Cl_2 and were then filtered using a glass fiber filter, which had been previously cleaned in the same manner as the pure mineral oxides. Subsequently, CH_2Cl_2 was evaporated and changed to 1.00 mL n-hexane under a gentle stream of nitrogen gas at 293 K.

Analyses of PAHs samples were performed by a GC–MS. The column was an HP 5MS (30 m \times 0.25 mm i.d. \times 0.25 μm film thickness). The methodology for the analysis of PAHs is similar to our previous study (Ma et al., 2010). 1.0 μL of each sample was introduced via EPC splitless mode injection. The injector temperature was 553 K. The oven temperature was held at 363 K for 2 min, then increased from 363 K to 603 K at a rate of 10 K min^{-1} and held at 603 K for 5 min. Helium was used as carrier gas at a constant flow of 1.5 mL min^{-1} . The interface temperature was kept at 553 K during analysis. For identification of the product, mass detection was performed in the scan mode (mass/charge ratio ranging from 50 to 500 a.u.), while for quantification of the reactant, mass detection was performed in selected ion monitoring (SIM) mode (dwell time = 10 ms, number of cycles per second = 12.3). The m/z ratio of 178 was used for quantification ion and the m/z ratio of 177 and 176 were used for confirmation ion for anthracene, respectively. The concentration of PAHs in solution was measured based on an external standard and the use of a calibration curve. The recovery obtained from spike and recovery experiments for anthracene on SiO_2 and MgO was $(95.6 \pm 3.51)\%$ and $(96.9 \pm 5.03)\%$, respectively. Therefore, GCMS areas were corrected for 100% recovery before quantification with the calibration curve.

The diffuse reflectance spectra were recorded on a NEXUS 6700 (Thermo Nicolet Instrument Corporation) FT-IR, equipped with an *in situ* diffuse reflection chamber and a high-sensitivity mercury cadmium telluride (MCT) detector cooled by liquid N_2 . The sample (about 11 mg) for the *in situ* DRIFTS studies was finely ground and placed into a ceramic crucible in the *in situ* chamber. The total flow rate was 100 mL min^{-1} , and the concentration of NO_2 was 4.43×10^{15} molecules cm^{-3} . Mineral oxides or mineral oxides coated with anthracene are used as the background to get the absorption spectra. The reference spectrum was measured in a synthesized air stream at 298 K. All spectra reported were recorded at a resolution of 4 cm^{-1} for 100 scans.

A UV–vis absorption spectrometer (U-3310 Spectrophotometer) was used to determine the absorption properties of the extract after the reaction. The samples were exposed to NO_2 at 298 K for 1 h and were then extracted and filtered using the same method mentioned above. Standard solution of anthracene in hexane was also prepared. Spectra were collected over a wavelength range of 190–650 nm at an interval of 1 nm and a scan speed of 600 nm min^{-1} .

2.4. Chemicals

All chemicals were chromatographic grade and used without further purification. CH_2Cl_2 and n-hexane were obtained from Baker Analyzed and Dima Technology Inc. Anthracene (99%), anthraquinone (99.5%), and 9-nitroanthracene (100 $\mu\text{g mL}^{-1}$ in Toluene) were purchased from Acros Organics, Dr. Ehrenstorfer GmbH, and AccuStandard Inc., respectively. Polynuclear aromatic hydrocarbon mix (the purity of anthracene was 100% and the prepared and certified analysis concentration of anthracene was 100 and 100.3 $\mu\text{g mL}^{-1}$, respectively), which was used as the standard for calibrations, was purchased from AccuStandard, Inc. High purity N_2 (99.99%) and O_2 (99.99%) were supplied by Beijing

AP BEIFEN Gases Inc. The experimental NO₂ was synthesized from the reaction between NO (1.03% + N₂, Beijing AP) and O₂.

3. Results and discussion

3.1. Characteristics of mineral oxides and surface coverage of anthracene

Table 1 shows the specific surface area of various substrates and the surface coverage (%) of anthracene used in experiments. In order to avoid the effect of anthracene surface coverage on the reaction, the same surface coverage on various substrates was used. Anthracene surface coverage was calculated by assuming that no aggregates were formed during the coating and that anthracene molecules were deposited horizontally beside each other (Perraudin et al., 2007). The cross section of anthracene molecule was assumed to be 1 nm² in calculations (Kwamena et al., 2006).

3.2. NO₂ reaction kinetics

3.2.1. The reaction on Teflon disc

Since Teflon is a sample cell and an inert material, the reaction on it was regarded as that of anthracene in unadsorbed form, i.e. the control experiment. As shown in Fig. 1, the concentration of anthracene decreased with increasing reaction time; however, within detection precision, the reaction of anthracene with NO₂ on Teflon disc can not be distinguished from the desorption of anthracene on it. As previously mentioned, Kwamena and Abbatt (2008) also revealed that anthracene and pyrene adsorbed on Teflon disc did not react with individual flows of NO₂ and HNO₃ at concentrations of 1 × 10¹³ and 7 × 10¹⁵ molecules cm⁻³, respectively.

3.2.2. Desorption study

To clarify that no desorption of anthracene was occurring during the reaction, blank experiments were performed under the same conditions as those used for the reactions (total darkness, air flow = 100 mL min⁻¹) but without NO₂. The concentrations of anthracene on particles purged with synthesized air over different lengths of time were almost the same as the initial concentration of anthracene adsorbed on mineral oxides (Fig. 2). The results show that, despite the relatively large vapor pressure of anthracene ($P = 1.0 \times 10^{-3}$ Pa at 298 K (Shiu and Ma, 2000)), the loss of anthracene by desorption was negligible under our experimental conditions and did not interfere significantly with kinetic measurements. Compared with the results in Fig. 1, it also means that the interaction between anthracene and mineral oxides was stronger than that between anthracene and Teflon disc.

3.2.3. Degradation kinetics of adsorbed anthracene and NO₂

The kinetics of the heterogeneous reaction between NO₂ and anthracene adsorbed on SiO₂ and MgO particles were determined by monitoring the loss of anthracene as a function of NO₂ exposure time at 298 K. The degradation of anthracene on SiO₂ and MgO

Table 1
Characteristics of mineral oxides and surface coverage of anthracene.

Samples	Specific surface area (m ² g ⁻¹)	An concentration (μg g ⁻¹)	An surface coverage (%)
SiO ₂	14.6	500	11.6
MgO	14.6	500	11.6
Teflon disc	3.39 cm ² ^a	1.16 μg ^b	11.6

^a The geometric surface area of the Teflon disc.

^b 1.16 μg per Teflon disc.

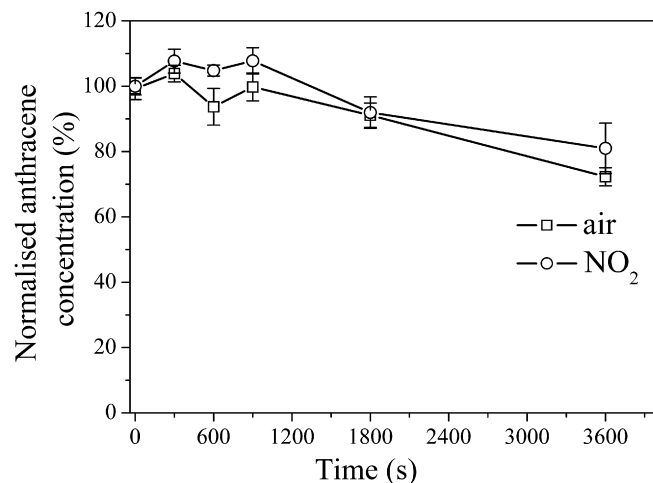


Fig. 1. Desorption and decay study for the anthracene adsorbed on Teflon disc (squares: loss by desorption; circles: loss by reaction with NO₂ and desorption) ($n = 3$, error bars represent 1 standard deviation).

showed an exponential pattern (Fig. 3), which suggests that the reactions are reasonably described by pseudo-first-order kinetics. Therefore, the experimental data were fitted using pseudo-first-order exponential functions (Perraudin et al., 2007) shown in equation (1),

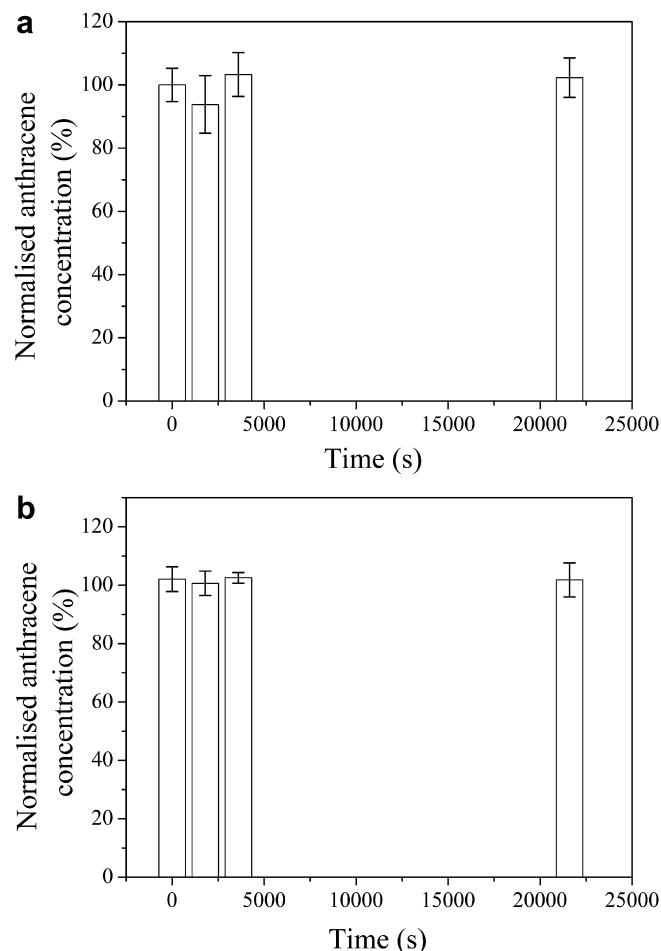


Fig. 2. Desorption study for the anthracene adsorbed on (a) SiO₂ and (b) MgO particles in air flow ($n = 3$, error bars represent 1 standard deviation).

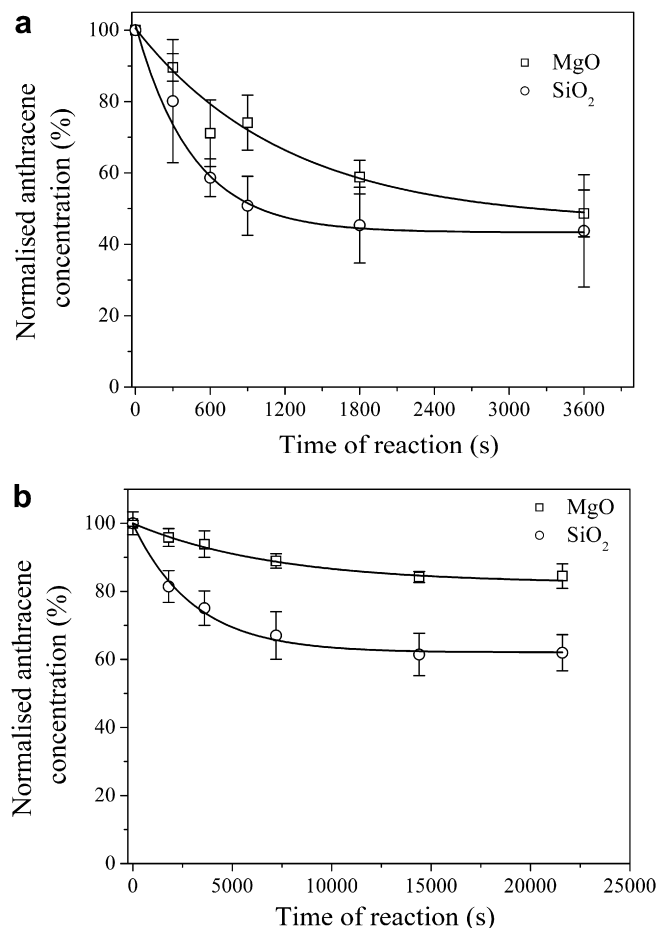


Fig. 3. Anthracene decays on various substrates in a flow of (a) 4.43×10^{15} molecules cm^{-3} and (b) 3.69×10^{12} molecules cm^{-3} $\text{NO} + 20\% \text{O}_2 + \text{N}_2$ at 298 K (squares: MgO; circles: SiO₂) ($n = 3$, error bars represent 1 standard deviation).

$$\frac{[\text{PAH}]_t}{[\text{PAH}]_0} = \frac{[\text{PAH}]_{\text{plateau}}}{[\text{PAH}]_0} + \frac{[\text{PAH}]_0 - [\text{PAH}]_{\text{plateau}}}{[\text{PAH}]_0} \times \exp(-k_{1,\text{obs}} \times t) \quad (1)$$

where $[\text{PAH}]_t$ is the concentration of adsorbed PAH at a given time, $[\text{PAH}]_0$ is the initial concentration of adsorbed PAH, $[\text{PAH}]_{\text{plateau}}$ is the concentration of adsorbed PAH at the plateau shown in Fig. 3, and $k_{1,\text{obs}}$ is the apparent rate constant of the pseudo-first-order reaction. The $k_{1,\text{obs}}$ values were $(2.92 \pm 1.47) \times 10^{-3} \text{ s}^{-1}$ on SiO₂ and $(1.06 \pm 0.50) \times 10^{-3} \text{ s}^{-1}$ on MgO when the concentration of NO₂ was 4.43×10^{15} molecules cm^{-3} . The reaction rate on SiO₂ was almost three times faster than on MgO. However, the concentration of NO₂ mentioned above is much higher than that relative to the atmosphere and there may be some N₂O₄ in equilibrium with NO₂. In order to exclude the possible effect of N₂O₄ on the reaction rate, additional experiment under lower concentration of NO₂ (3.69×10^{12} molecules cm^{-3}) was carried out. The $k_{1,\text{obs}}$ values were $(3.70 \pm 1.29) \times 10^{-4} \text{ s}^{-1}$ on SiO₂ and $(1.97 \pm 1.05) \times 10^{-4} \text{ s}^{-1}$ on MgO. The reaction rate on SiO₂ was almost two times faster than on MgO. Although the $k_{1,\text{obs}}$ was one order of magnitude lower than that under high NO₂ concentration, the $k_{1,\text{obs}}$ on SiO₂ was also higher than that on MgO. Therefore, the difference between the reaction rate on SiO₂ and MgO was not caused by the effect of N₂O₄. In order to increase the signal to noise ratio, higher concentration of NO₂ was used for product and mechanism studies. There was only one report of the $k_{1,\text{obs}}$ for the reaction of NO₂ with anthracene

adsorbed on SiO₂ under lower concentration of NO₂ (1.5×10^{12} molecules cm^{-3}) and lower pressure ($240 \pm 15 \text{ Pa}$), and the $k_{1,\text{obs}}$ was comparable with the values under lower concentration of NO₂ (3.69×10^{12} molecules cm^{-3}) measured in our study (Perraudin et al., 2005). As seen in Fig. 3, the reaction of NO₂ with anthracene was not completed on these mineral substrates. Esteve et al. (2004) found that the plateau was about 54% for the reaction of NO₂ with anthracene adsorbed on graphite particles. Many hypotheses were put forward to explain the presence of such a plateau. One possibility is that anthracene was not deposited as a smooth, uniform layer, but more likely as clumps or islands even in a submonolayer regime (Esteve et al., 2004). Therefore, the reaction products with lower vapor pressure may be adsorbed on the molecules of anthracene, and then prevent the further reaction of anthracene in the sublayers. Additionally, a poor diffusion of NO₂ through the particle layers could limit the consumption of PAHs.

3.3. Product and mechanism study

3.3.1. In situ DRIFTS study

In order to investigate the effects of the mineral substrates on the heterogeneous reactions of PAHs with NO₂, *in situ* DRIFTS experiments were performed in a flow system. The infrared spectra of pure SiO₂ particles in a flow of NO + O₂ are shown in Fig. 4a. Only two peaks at 1628 and 1602 cm^{-1} became predominant with increasing exposure time, which disappeared immediately when the sample was purged with synthesized air. These two peaks were assigned to the gas-phase of NO₂ (Goodman et al., 1999). As shown in Fig. 4a, no peaks attributing to surface nitrate were observed. The spectrum is similar to the results reported by Goodman et al. (1999) where dehydrated SiO₂ was exposed to pure NO₂. Our previous work has indicated that NO with excess O₂ can be used as a substitute of pure NO₂ (Ma et al., 2008). It should be pointed out that Goodman et al. (1999) observed the formation of adsorbed nitric acid when gaseous NO₂ reacts with SiO₂ at a relative humidity of 4%. Because the remnant water in the nitrogen stream can not be removed completely in the flow system at room temperature (RH ≈ 3.7%), nitric acid should also be formed on SiO₂ in this work. However, the peaks of nitric acid were not observed in the infrared spectra due to their low concentration on the surface. To confirm the formation of nitric acid on SiO₂, the infrared spectra for the adsorption of NO + O₂ on SiO₂ with high specific surface area ($420 \text{ m}^2 \text{ g}^{-1}$) are shown in Fig. 4b. The peaks at 1676 and 1312 cm^{-1} ascribed to adsorbed nitric acid (Goodman et al., 1999) were observed clearly when the concentration of NO was higher than 4.43×10^{15} molecules cm^{-3} .

The infrared spectra for the heterogeneous reaction between NO₂ and anthracene adsorbed on SiO₂ are shown in Fig. 4c. The negative peaks at 3051, 1620, 956, and 883 cm^{-1} revealed the consumption of anthracene (Hudgins and Sandford, 1998; Cané et al., 1997). The bands at 1556 and 1524 cm^{-1} are the characteristic frequency of 9-nitroanthracene (Kwamena and Abbatt, 2008). The bands at 3066, 1669, 1588, and 1537 cm^{-1} are assigned to 9,10-anthraquinone (Ball et al., 1996). The absorption of 9,10-anthraquinone and 9-nitroanthracene from 1200 to 1500 cm^{-1} could not be clearly observed due to the strong SiO₂ lattice absorption (data not shown). These results suggest that the heterogeneous reaction between NO₂ and anthracene adsorbed on SiO₂ leads to the formation of 9-nitroanthracene and 9,10-anthraquinone.

The infrared spectra of pure MgO particles in a flow of NO + O₂ are shown in Fig. 5a. Several bands at the 1800–900 cm^{-1} region became predominant with increasing exposure time. These bands can be assigned to oxide-coordinated, water-solvated and ion-coordinated nitrates (Ma et al., 2008; Underwood et al., 1999; Miller and Grassian, 1998; Goodman et al., 2001). The bands at 1222 and

1308 cm^{-1} are assigned to the ν_3 and ν_1 modes of a chelating bidentate nitrite species, respectively (Ma et al., 2008; Underwood et al., 1999; Miller and Grassian, 1998). The intensities of these bands initially grew, attained its maximum within a few minutes, and then decreased with the increasing of time. It is suggested

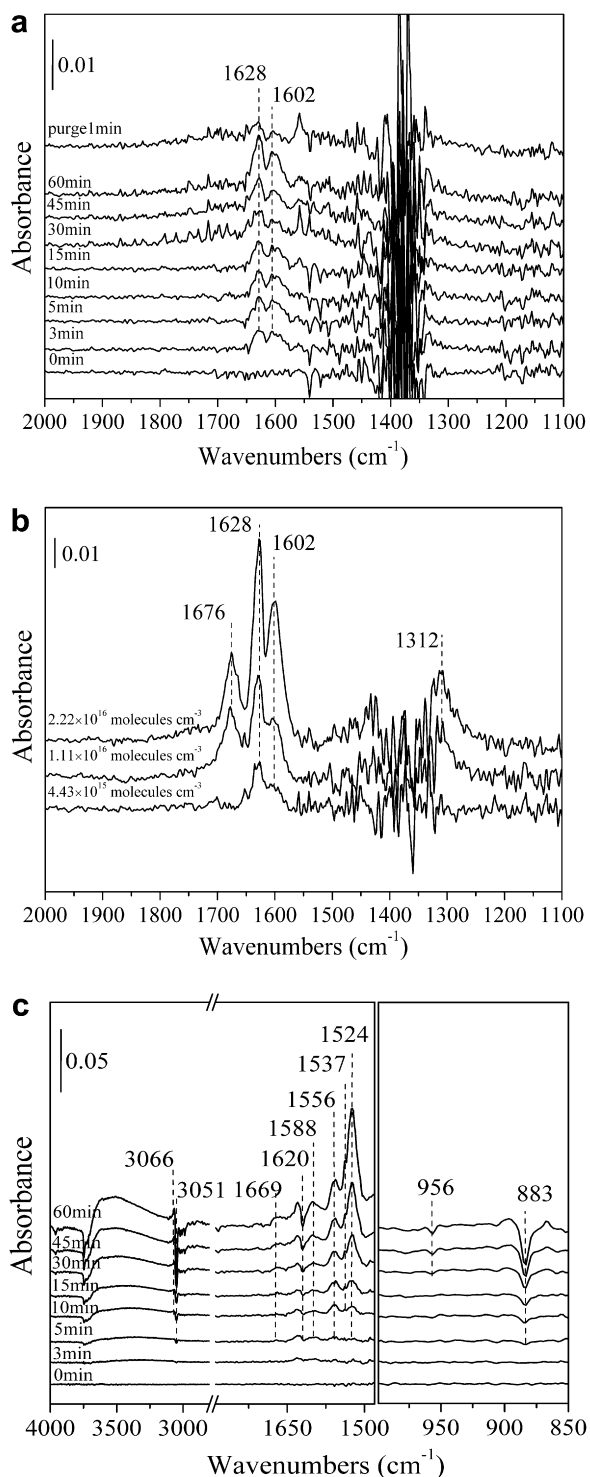


Fig. 4. *In situ* DRIFTS spectra of (a) pure SiO₂ (14.6 m² g⁻¹) as a function of time (0, 3, 5, 10, 15, 30, 45, 60 min) in a flow of 4.43×10^{15} molecules cm⁻³ NO + 20% O₂ + N₂ at 298 K; (b) SiO₂ (420 m² g⁻¹) exposed to a flow of NO + 20% O₂ + N₂ with different concentration of NO for 10 min at 298 K; and (c) anthracene adsorbed on SiO₂ (14.6 m² g⁻¹, 1%wt of anthracene) as a function of time (0, 3, 5, 10, 15, 30, 45, 60 min) in a flow of 4.43×10^{15} molecules cm⁻³ NO + 20% O₂ + N₂ at 298 K.

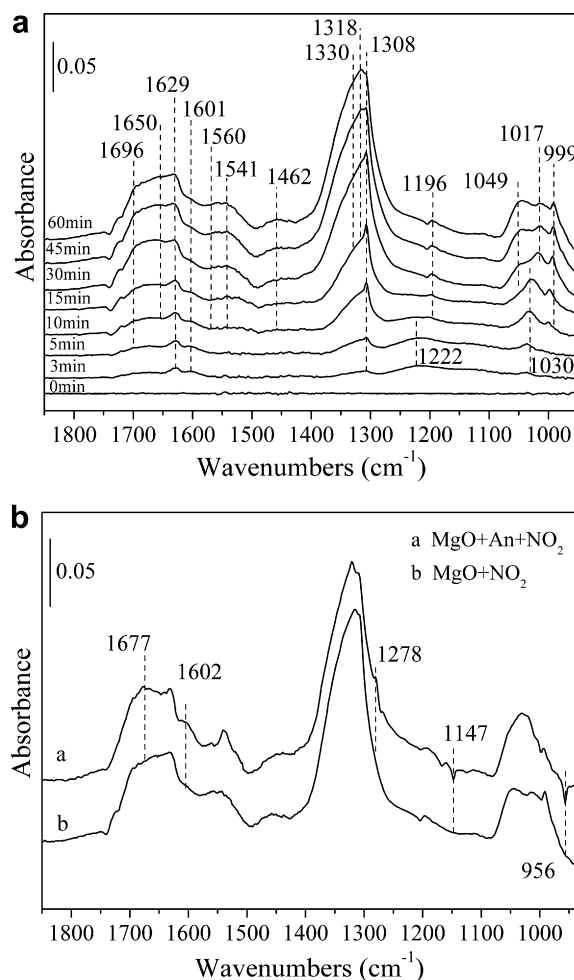


Fig. 5. (a) *In situ* DRIFTS spectra of pure MgO as a function of time (0, 3, 5, 10, 15, 30, 45, 60 min) in a flow of 4.43×10^{15} molecules cm⁻³ NO + 20% O₂ + N₂ at 298 K. (b) Comparative of the spectra of anthracene adsorbed on MgO (1%wt) and MgO exposed to a flow of 4.43×10^{15} molecules cm⁻³ NO + 20% O₂ + N₂ at 298 K for 60 min.

bidentate nitrite is the intermediate in the conversion of adsorbed NO₂ to nitrate. Because the remnant water in the nitrogen stream can not be removed completely in the flow system at room temperature (RH ≈ 3.7%), adsorption due to water-solvated surface nitrate at 1308 cm^{-1} is apparent (Ma et al., 2008; Underwood et al., 1999; Miller and Grassian, 1998). The band at 1629 cm^{-1} is assigned to the bending mode of adsorbed water. The bands at 1650 and 1196 cm^{-1} are ascribed to the degenerate ν_3 mode of oxide-coordinated bridging nitrate, and the bands at 1541 and 1462 cm^{-1} are assigned to the degenerate ν_3 mode of oxide-coordinated monodentate nitrate, which have been split into two bands due to a loss of symmetry upon adsorption. The band at 1560 cm^{-1} is assigned to the ν_3 mode of oxide-coordinated bidentate nitrate. Because the water-solvated nitrate and oxide-coordinated nitrate bands overlap in the 1308 cm^{-1} region, the lower energy split of the ν_3 mode of the bidentate nitrate species could not be clearly discriminated. The bands in the $1100\text{--}900\text{ cm}^{-1}$ region are assigned to the ν_1 mode of adsorbed nitrate. The strongest bands at 1318 and 1330 cm^{-1} are the characteristic frequency of ion-coordinated nitrate (Goodman et al., 2001). Thus, as NO₂ reacted with MgO, not only surface nitrate but also bulk Mg(NO₃)₂ were formed; while no adsorbed nitric acid was formed on MgO, even under higher concentration of NO (data not shown). This is consistent with the results reported by Goodman et al. (2001) where MgO was exposed to nitric acid.

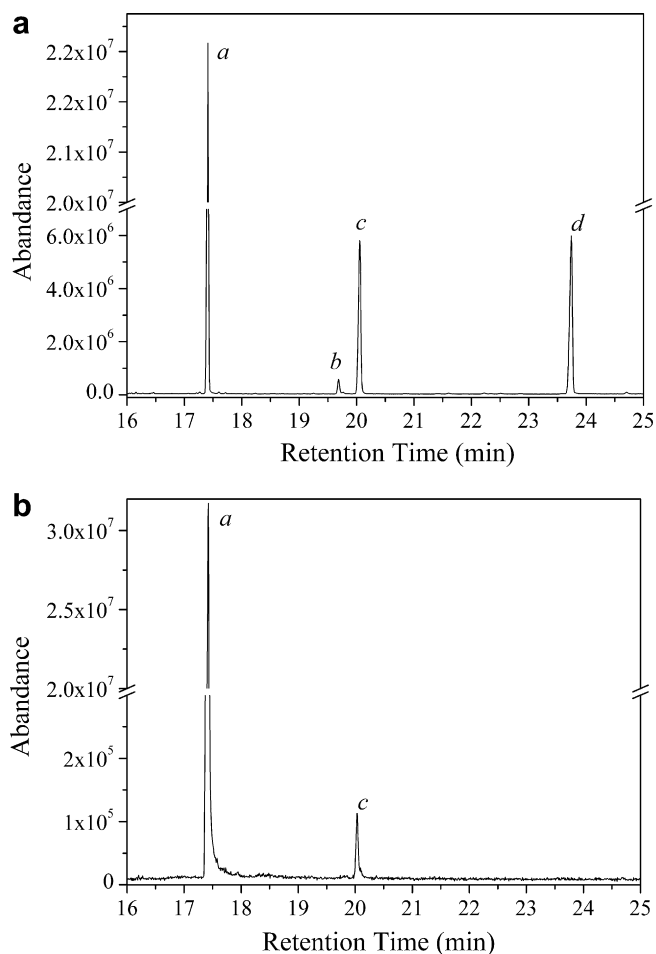


Fig. 6. Total ion chromatogram (TIC) of nitration products of anthracene adsorbed on (a) SiO₂ and (b) MgO.

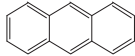
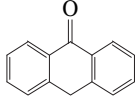
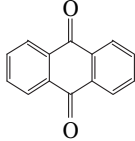
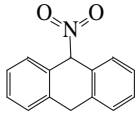
The infrared spectra for the heterogeneous reaction between NO₂ and anthracene adsorbed on MgO are shown in Fig. 5b. The negative peaks at 1147 and 956 cm⁻¹ (Hudgins and Sandford, 1998; Cané et al., 1997) showed the decrease of anthracene on the MgO surface. The bands at 1677, 1602, and 1278 cm⁻¹ are assigned to 9,10-anthraquinone (Ball et al., 1996). These results suggest that the heterogeneous reaction between NO₂ and anthracene adsorbed on MgO only leads to the formation of 9,10-anthraquinone.

In situ DRIFTS results suggest that the difference in the kinetic and reaction pathways for the heterogeneous reaction between NO₂ and anthracene adsorbed on mineral oxides could be ascribed to the formation of HNO₃, which can catalyze the nitration of PAHs by NO₂ (Pitts et al., 1978; Ramdahl and Bjørseth, 1984; Wang et al., 1999, 2000a,b). Nitric acid formed on the acidic SiO₂ surface, and thus explains the high reactivity of PAHs on this surface. Conversely, nitric acid was not formed on the MgO surface and a corresponding lower reactivity was observed in our experiment.

3.3.2. GCMS study

GCMS analysis was performed to conclusively identify specific products of the heterogeneous nitration of surface-bound anthracene, i.e., those that can be extracted and pass through the GC column. Total ion chromatogram (TIC) of the nitration products of anthracene adsorbed on SiO₂ and MgO are presented in Fig. 6. Peak *a* in the gas chromatogram was anthracene. Peak *b*, *c* and *d* were the reaction products and were analyzed in detail by mass

Table 2
Results of products analysis.

Peak	Name	structure	Fit (%) of NIST library
<i>a</i>	Anthracene		93
<i>b</i>	Anthrone		94
<i>c</i>	9,10-Anthraquinone		98
<i>d</i>	9-Nitroanthracene		99

spectroscopy. The product identification was carried out by comparing the mass spectra of the obtained product with those from the mass spectra library. Table 2 shows the results of identified products. Additionally, 9,10-anthraquinone and 9-nitroanthracene were confirmed by the spectra of standard samples. The only mononitrated product formed by NO₂ reaction with anthracene adsorbed on SiO₂ was 9-nitroanthracene, probably due to the favorable nucleophilic position of -9. This is consistent with results of electrophilic nitration, in which the nitration of anthracene by NO₂ in dichloromethane produced 9,10-anthraquinone and 9-nitroanthracene (Pryor et al., 1984). The formation of anthrone and 9,10-anthraquinone in this work may also result from the trapping of the anthracene radical-cation intermediate by water, as suggested by Pryor et al. (1984).

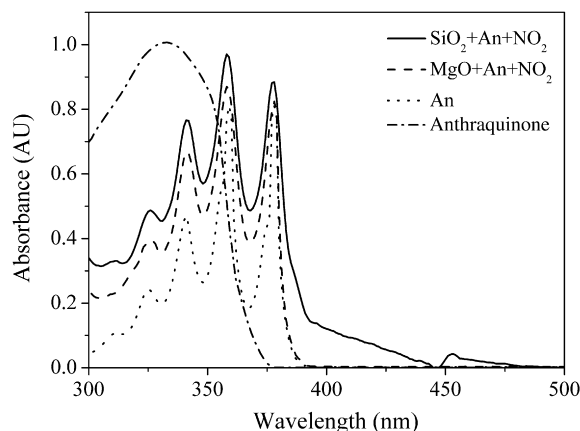


Fig. 7. Absorption spectra of anthracene before and after exposure to NO₂ on SiO₂ and MgO (Solid line, spectrum of anthracene react with NO₂ on SiO₂; Dashed line, spectrum of anthracene react with NO₂ on MgO; Dotted line, spectrum of anthracene; Dash Dotted line, spectrum of anthraquinone).

3.3.3. UV–vis study

UV–vis absorption experiments were performed to determine how the reactions alter the optical properties of the extract. As shown in Fig. 7, anthracene and 9,10-anthraquinone do not absorb visible light. The absorption in the visible portion of the spectrum can be assigned to 9-nitroanthracene (Kwamena and Abbatt, 2008). The enhancement of absorption in the UV portion of the spectrum on SiO₂ was due to the formation of 9-nitroanthracene and 9,10-anthraquinone. The enhancement of absorption in the UV portion of the spectrum on MgO was due to the formation of 9,10-anthraquinone (Fidder et al., 2009). Due to the formation of these products, the heterogeneous reactions of NO₂ with anthracene might alter the optical properties of the mineral oxides on which anthracene were adsorbed.

4. Conclusions

In this study, heterogeneous reactions of NO₂ with anthracene adsorbed on SiO₂ and MgO were investigated under dark conditions at room temperature. Within our experimental detection limit, no reaction between NO₂ and anthracene on Teflon disc was observed. The apparent reaction rate on SiO₂ was almost two times faster than that on MgO when the concentration of NO₂ was 3.69×10^{12} molecules cm⁻³. Both 9-nitroanthracene and 9,10-anthraquinone were the products of the nitration of anthracene adsorbed on SiO₂, whereas 9,10-anthraquinone was the only product formed by the NO₂ reaction with anthracene adsorbed on MgO. These results suggest that mineral oxides not only alter kinetics but also the reaction pathway for the heterogeneous reaction of PAHs with NO₂. *In situ* DRIFTS results indicate that the difference in the kinetic and reaction pathways for the heterogeneous reaction between NO₂ and anthracene adsorbed on mineral oxides was ascribed to the formation of HNO₃, which catalyzed the nitration of PAHs by NO₂. As we know, SiO₂ is the main composition of mineral dust (about 60% wt). The heterogeneous reaction of NO₂ with PAHs adsorbed on mineral dust must be taken into account when considering the source of nitro-PAHs in the atmosphere and the toxicity of atmospheric particles.

Acknowledgements

This research was funded by the Ministry of Science and Technology, China (2007CB407301), the National Natural Science Foundation of China (20937004, 20907069), and the National Scientific and Technological special program of Commonweal industry (200809087).

References

Albinet, A., Leoz-Garziandia, E., Budzinski, H., Villenave, E., 2006. Simultaneous analysis of oxygenated and nitrated polycyclic aromatic hydrocarbons on standard reference material 1649a (urban dust) and on natural ambient air samples by gas chromatography-mass spectrometry with negative ion chemical ionisation. *Journal of Chromatography A* 1121, 106–113.

Atkinson, R., Arey, J., 1994. Atmospheric chemistry of gas-phase polycyclic aromatic hydrocarbons: formation of atmospheric mutagens. *Environmental Health Perspective* 102, 117–126.

Atkinson, R., Arey, J., Zielinska, B., Aschmann, S.M., 1987. Kinetics and products of the gas-phase reactions of OH radicals and N₂O₅ with naphthalene and biphenyl. *Environmental Science and Technology* 21, 1014–1022.

Ball, B., Zhou, X.F., Liu, R.F., 1996. Density functional theory study of vibrational spectra. 8. Assignment of fundamental vibrational modes of 9,10-anthraquinone and 9,10-anthraquinone-d₈. *Spectrochimica Acta Part A – Molecular and Biomolecular Spectroscopy* 52, 1803–1814.

Bunce, N.J., Liu, L., Zhu, J., 1997. Reaction of naphthalene and its derivatives with hydroxyl radicals in the gas phase. *Environmental Science and Technology* 31, 2252–2259.

Calvert, J.G., Atkinson, R., Becker, K.H., Kamens, R.M., Seinfeld, J.H., Wallington, T.J., Yarwood, G., 2002. *The Mechanisms of Atmospheric Oxidation of Aromatic Hydrocarbons*. Oxford University Press, Oxford.

Cané, E., Miani, A., Palmieri, P., Tarroni, R., Trombetti, A., 1997. The gas-phase infrared spectra of anthracene-h₁₀ and anthracene-d₁₀. *Journal of Chemical Physics* 106, 9004–9012.

Dentener, F.J., Carmichael, G.R., Zhang, Y., Lelieveld, J., Crutzen, P.J., 1996. Role of mineral aerosol as a reactive surface in the global troposphere. *Journal of Geophysical Research* 101, 22869–22889.

Esteve, W., Budzinski, H., Villenave, E., 2004. Relative rate constants for the heterogeneous reactions of OH, NO₂ and NO radicals with polycyclic aromatic hydrocarbons adsorbed on carbonaceous particles. Part 1: PAHs adsorbed on 1–2 μm calibrated graphite particles. *Atmospheric Environment* 38, 6063–6072.

Esteve, W., Budzinski, H., Villenave, E., 2006. Relative rate constants for the heterogeneous reactions of NO₂ and OH radicals with polycyclic aromatic hydrocarbons adsorbed on carbonaceous particles. Part 2: PAHs adsorbed on diesel particulate exhaust SRM 1650a. *Atmospheric Environment* 40, 201–211.

Feilberg, A., 2000. *Atmospheric Chemistry of Polycyclic Aromatic Compounds with Special Emphasis on Nitro Derivatives*. Ph.D. thesis, Risø National Laboratory, Denmark.

Feilberg, A., Poulsen, M.W.B., Nielsen, T., Skov, H., 2001. Occurrence and sources of particulate nitro-polycyclic aromatic hydrocarbons in ambient air in Denmark. *Atmospheric Environment* 35, 353–366.

Fidder, H., Lauer, A., Freyer, W., Koeppe, B., Heyne, K., 2009. Photochemistry of anthracene-9,10-endoperoxide. *Journal of Physical Chemistry A* 113, 6289–6296.

Finlayson-Pitts, B.J., Pitts Jr., J.N., 1997. Tropospheric air pollution: ozone, airborne toxics, polycyclic aromatic hydrocarbons, and particles. *Science* 276, 1045–1052.

Fu, S., Li, K., Xia, X.J., Xu, X.B., 2009. Polycyclic aromatic hydrocarbons residues in sandstorm depositions in Beijing, China. *Bulletin of Environmental Contamination and Toxicology* 82, 162–166.

Goodman, A.L., Bernard, E.T., Grassian, V.H., 2001. Spectroscopic study of nitric acid and water adsorption on oxide particles: enhanced nitric acid uptake kinetics in the presence of adsorbed water. *Journal of Physical Chemistry A* 105, 6443–6457.

Goodman, A.L., Underwood, G.M., Grassian, V.H., 1999. Heterogeneous reaction of NO₂: characterization of gas-phase and adsorbed products from the reaction, 2NO₂(g) + H₂O(a) → HONO(g) + HNO₃(a) on hydrated silica particles. *Journal of Physical Chemistry A* 103, 7217–7223.

Hudgins, D.M., Sandford, S.A., 1998. Infrared spectroscopy of matrix isolated polycyclic aromatic hydrocarbons. 1. PAHs containing two to four rings. *Journal of Physical Chemistry A* 102, 329–343.

Kamens, R.M., Guo, J.Z., Guo, Z.S., McDow, S.R., 1990. Polynuclear aromatic hydrocarbon degradation by heterogeneous reactions with N₂O₅ on atmospheric particles. *Atmospheric Environment* 24A, 1161–1173.

Kwamena, N.O.A., Abbatt, J.P.D., 2008. Heterogeneous nitration reactions of polycyclic aromatic hydrocarbons and n-hexane soot by exposure to NO₃/NO₂/N₂O₅. *Atmospheric Environment* 42, 8309–8314.

Kwamena, N.O.A., Earp, M.E., Young, C.J., Abbatt, J.P.D., 2006. Kinetic and product yield study of the heterogeneous gas-surface reaction of anthracene and ozone. *Journal of Physical Chemistry A* 110, 3638–3646.

Ma, J.Z., Liu, Y.C., He, H., 2010. Degradation kinetics of anthracene by ozone on mineral oxides. *Atmospheric Environment* 44, 4446–4453.

Ma, Q.X., Liu, Y.C., He, H., 2008. Synergistic effect between NO₂ and SO₂ in their adsorption and reaction on γ-alumina. *Journal of Physical Chemistry A* 112, 6630–6635.

Miller, T.M., Grassian, V.H., 1998. Heterogeneous chemistry of NO₂ on mineral oxide particles: spectroscopic evidence for oxide-coordinated and water-solvated surface nitrate. *Geophysical Research Letters* 25, 3835–3838.

Onchoke, K.K., Parks, M.E., Nolan, A.H., 2009. A DFT study of the vibrational spectra of 1- and 2-nitrotriphenylene. *Spectrochimica Acta Part A* 74, 579–587.

Perraudin, E., Budzinski, H., Villenave, E., 2005. Kinetic study of the reactions of NO₂ with polycyclic aromatic hydrocarbons adsorbed on silica particles. *Atmospheric Environment* 39, 6557–6567.

Perraudin, E., Budzinski, H., Villenave, E., 2007. Kinetic study of the reactions of ozone with polycyclic aromatic hydrocarbons adsorbed on atmospheric model particles. *Journal of Atmospheric Chemistry* 56, 57–82.

Pitts Jr., J.N., Sweetman, J.A., Zielinska, B., Winer, A.M., Atkinson, R., 1985a. Determination of 2-nitrofluoranthene and 2-nitropyrene in ambient particulate organic matter: evidence for atmospheric reactions. *Atmospheric Environment* 19, 1601–1608.

Pitts Jr., J.N., Van Cauwenberghe, K.A., Grosjean, D., Schmid, J.P., Fitz, D.R., Belser Jr., W.L., Knudson, G.B., Hynds, P.M., 1978. Atmospheric reactions of polycyclic aromatic hydrocarbons: facile formation of mutagenic nitro derivatives. *Science* 202, 515–519.

Pitts Jr., J.N., Zielinska, B., Sweetman, J.A., Atkinson, R., Winer, A.M., 1985b. Reactions of adsorbed pyrene and perylene with gaseous N₂O₅ under simulated atmospheric conditions. *Atmospheric Environment* 19, 911–915.

Pryor, W.A., Gleicher, G.J., Cosgrove, J.P., Church, D.F., 1984. Reaction of polycyclic aromatic hydrocarbons (PAH) with nitrogen dioxide in solution. Support for an electron-transfer mechanism of aromatic nitration based on correlations using simple molecular orbital theory. *Journal of Organic Chemistry* 49, 5189–5194.

Ramdahl, T., Bjørseth, A., 1984. Nitration of polycyclic aromatic hydrocarbons adsorbed to different carriers in a fluidized bed reactor. *Chemosphere* 13, 527–534.

Ramdahl, T., Zielinska, B., Arey, J., Atkinson, R., Winer, A.M., Pitts Jr., J.N., 1986. Ubiquitous occurrence of 2-nitrofluoranthene and 2-nitropyrene in air. *Nature* 321, 425–427.

- Shiu, W.Y., Ma, K.C., 2000. Temperature dependence of physical-chemical properties of selected chemicals of environmental interest. I. Mononuclear and polynuclear aromatic hydrocarbons. *Journal of Physical and Chemical Reference Data* 29, 41–130.
- Underwood, G.M., Miller, T.M., Grassian, V.H., 1999. Transmission FT-IR and Knudsen cell study of the heterogeneous reactivity of gaseous nitrogen dioxide on mineral oxide particles. *Journal of Physical Chemistry A* 103, 6184–6190.
- Wang, H.W., Hasegawa, K., Kagaya, S., 1999. Nitration of pyrene adsorbed on silica particles by nitrogen dioxide under simulated atmospheric conditions. *Chemosphere* 39, 1923–1936.
- Wang, H.W., Hasegawa, K., Kagaya, S., 2000a. The nitration of pyrene adsorbed on silica particles by nitrogen dioxide. *Chemosphere* 41, 1479–1484.
- Wang, H.W., Hasegawa, K., Kagaya, S., 2000b. Effect of nitrous acid gas on the nitration of pyrene adsorbed on silica particles by nitrogen dioxide. *Journal of Environmental Science and Health, Part A Toxic/Hazardous Substances and Environmental Engineering* 35, 765–773.
- Wu, C.H., Niki, H., 1985. Fluorescence spectroscopic study of kinetics of gas-surface reactions between nitrogen dioxide and adsorbed pyrene. *Environmental Science and Technology* 19, 1089–1094.
- Wu, S.P., Tao, S., Xu, F.L., Dawson, R., Lan, T., Li, B.G., Cao, J., 2005. Polycyclic aromatic hydrocarbons in dustfall in Tianjin, China. *Science of Total Environment* 345, 115–126.
- Xu, X.B., Jin, Z.L., 1984. High-performance liquid-chromatographic studies of environmental carcinogens in china. *Journal of Chromatography* 317, 545–555.